Available online at www.sciencedirect.com
SCIENCE DIRECT
Catalysis Today 116 (2006) 111–120
CATALYSIS TODAY
www.elsevier.com/locate/cattod

A solid-state NMR, FT-IR and TPD study on acid properties of sulfated and metal-promoted zirconia: Influence of promoter and sulfation treatment

Wen-Hua Chen [a], Hui-Hsin Ko [a], Ayyamperumal Sakthivel [a,1], Shing-Jong Huang [a], Shou-Heng Liu [a], An-Ya Lo [a], Tseng-Chang Tsai [b], Shang-Bin Liu [a,*]

[a] *Institute of Atomic and Molecular Sciences, Academia Sinica, PO Box 23-166, Taipei, Taiwan 106, ROC*
[b] *Department of Applied Chemistry, National University of Kaohsiung, Kaohsiung, Taiwan 811, ROC*

Available online 23 May 2006

Abstract

The acid properties of various sulfated and metal-promoted zirconium oxide (ZrO_2) catalysts have been studied by solid-state ^{31}P MAS NMR, FT-IR and TPD using the adsorbed trimethylphosphine oxide (TMPO), pyridine and ammonia as the probe molecule, respectively. Sulfated zirconia (SZ) catalysts having varied sulfur contents and metal promoter (M = Al, Ga and Fe) were prepared by sol–gel method. Effects of sulfation and promoter on the detailed qualitative and quantitative information of acid sites, viz. types (Brønsted versus Lewis), strengths and distributions, on various synthesized SZ and M/SZ were examined by ^{31}P MAS NMR of adsorbed TMPO in conjunction with elemental analyses by ICP-MS. By comparison, pyridine-IR and NH_3-TPD methods are capable of providing only qualitative information of the overall acidity. It was found that while the parent ZrO_2 possesses only weak Lewis acidities, elaborated sulfation treatment leads to formation and coexistence of strong Brønsted (B) and Lewis (L) acid sites whose variations can readily be followed. On the other hand, incorporation of different metal promoters onto SZ, led to simultaneous formation/elimination and variations of B- and L-sites with varied strengths and distributions. As a result, Ga/SZ was found to possess more B- than L-sites, whereas an opposite trend was observed for Al/SZ. As for Fe/SZ, a pronounced increase in both concentration and strength of acid sites were found. With an exception of Ga/SZ, the 'very strong' acid sites observed for various SZ and M/SZ catalysts were found to be associated more to L- than B-sites.

Keywords: Sulfated zirconia; Metal promoter; Acidity; Solid-state ^{31}P NMR; Pyridine-IR; NH_3-TPD

1. Introduction

Sulfated zirconia (SO_4^{2-}–ZrO_2; SZ) is an environmental-friendly and practical solid acid catalyst commonly used in industrial processes, especially those invoking low-temperature conversion of hydrocarbons, such as hydroisomerization, hydrocracking, alkylation, esterification, cyclization, etc. [1–4]. However, SZ is also known as a catalyst vulnerable to rapid deactivation. This drawback is normally circumvented by adding suitable amount of metal promoter, such as Pt, Al, Ga, Fe or Mn. Consequently, metal-promoted SZ (M/SZ) catalysts were mostly found to engender both Brønsted and Lewis acidities with superior acid strengths. As such, M/SZ's are also known as 'superacid' catalysts renderable for exceptional activity and selectivity during hydrocarbon conversion reactions, e.g., *n*-butane isomerization [5–15]. Nevertheless, the strengths and types of acid sites of SZ deserve further justification; while most of the existing literatures [1–18] revealed that calcination treatment at elevated temperatures tends to promote the co-existence of Brønsted and Lewis acid sites, whose acidic strengths are much higher than typical solid acid catalysts, such as zeolites. On the other hand, some reports [19–21] questioned the existence of 'superacidity' in SZ catalysts and claimed that the strength of Brønsted acid sites in SZ are only comparable and, in some cases, even weaker than typical zeolitic catalysts, such as H-X, H-Y or H-ZSM-5. Similar arguments prevail regarding to the promoting effects of metals on acidity of SZ [9,12–15,19–26]. Thus, the nature and

* Corresponding author. Tel.: +886 2 23668230; fax: +886 2 23620200.
E-mail address: sbliu@sinica.edu.tw (S.-B. Liu).
[1] Present address: Anorganisch-Chemisches Institut, Technische Universität München, Litchtenbergstr.4, D-85747 Garching, Germany.

0920-5861/$ – see front matter © 2006 Elsevier B.V. All rights reserved.
doi:10.1016/j.cattod.2006.01.025

acidic features of acid sites in SZ and M/SZ catalysts remain as debatable issues for which this report aims to justify.

In terms of acidity characterization of solid acid catalysts, conventional methods normally invoke either direct observation of the acidic hydroxyl OH groups by using IR and/or ^{1}H NMR spectroscopy or through the adsorption of suitable basic probe molecules (mostly containing elements with unpaired electrons, such as N, O, P, etc.) followed by analytical and/or spectroscopic techniques, such as titration, temperature-programmed desorption (TPD), calorimetry and infrared (IR) or nuclear magnetic resonance (NMR) spectroscopy [27]. Nonetheless, while some of the above methods are useful in providing qualitative information (e.g., acid types) of the acid sites, most techniques are capable of providing only quantitative (acid amount and/or strength) information regarding to the *overall* acidity of solid acid catalysts. In this context, numerous reports on acidity characterization of SZ and assorted M/SZ catalysts can be found using the aforementioned conventional techniques [17–26,28–42]. A novel solid-state ^{31}P magic-angle-spinning (MAS) NMR technique developed recently using trialkylphosphine oxides as probe molecules, however, reveals the propensity in providing detailed acid features, namely the types (Brønsted versus Lewis acidity), concentrations (distributions and amounts) and strength of acid sites in solid acid catalysts simultaneously [27,43–45]. In particular, when applied in conjunction with elemental analysis (e.g., by inductively coupled plasma mass spectrometry; ICP-MS) and with proper choices of phosphine oxide probe molecules having varied sizes, e.g., trimethylphosphine oxide (TMPO; kinetic diameter ca. 0.55 nm) or tributylphosphine oxide (TBPO; size ca. 0.82 nm), additional qualitative and quantitative information, such as the amount and location (internal versus external) of acid sites can also be inferred by the ^{31}P MAS NMR spectroscopy [27], as illustrated previously for various solid acid catalysts [45–47].

In this study, the properties and variations of acid sites on various SZ and M/SZ catalysts with varied sulfur contents and promoted metal (Al, Ga and Fe) loadings were investigated by means of solid-state ^{31}P MAS NMR of the adsorbed TMPO and ICP-MS. The results were further compared with those obtained from conventional pyridine-IR and ammonia temperature-programmed desorption (NH_3-TPD) experiments.

2. Experimental

2.1. Catalyst preparation

SZ catalysts with varied sulfur contents were prepared according to a colloidal sol–gel method reported earlier by Sakthivel et al. [48]. First of all, zirconium hydride $Zr(OH)_4$ was synthesized by dissolving ca. 50 g of zirconium oxy chloride hydride ($ZrOCl_2{\cdot}8H_2O$; Acros) in 400 mL distilled water at 343 K, followed by precipitation with ammonium hydroxide (NH_4OH; Acros) solution controlled at a pH of ca. 9.1–9.3. The precipitated $Zr(OH)_4$ was repeatedly washed with distilled water till free of chloride and ammonium ions (using $AgNO_3$ as test reagent; Merck), dried at 373–383 K for 24 h, then grinded into fine powder. Subsequently, ca. 1 g of $Zr(OH)_4$ sample was treated with 15 mL of sulfuric acid (H_2SO_4; Acros) having desirable concentrations (0.5, 1.0 and 2.0N), stirred for 15–20 min, then filtered without washing. The sample was then dried at 373 K for 12 h, followed by calcination in air at 873 K for 3 h. These samples are hereafter denoted as SZ-*x*N, where $x = 0.5$, 1.0 and 2.0 represents the concentration of sulfuric acid added during the sulfation treatment. The Al_2O_3 and Ga_2O_3 promoted SZ-1.0N samples (denoted as Al/SZ and Ga/SZ, respectively) were prepared by the aforedescribed procedures except that during the initial step, ca. 0.91 g of aluminum ($Al(NO_3)_3{\cdot}9H_2O$; Merck) or 0.63 g gallium nitrate ($Ga(NO_3)_3{\cdot}9H_2O$; Acros) was added along with the $ZrOCl_2{\cdot}8H_2O$ solution [36]. On the other hand, Fe_2O_3 promoted SZ-1.0N catalyst (denoted as Fe/SZ) was prepared by adding ca. 1 g of as-prepared SZ sample into 25 mL of iron(III) nitrate ($Fe(NO_3)_3{\cdot}9H_2O$; Acros) solution [49], stirred for 0.5 h, filtered without washing, then dried at 373 K for 1 day. Finally, the sample was calcined in air at 873 K for 3 h (at a heating rate of 5 K/min).

The structural features of the parent ZrO_2, SZ and M/SZ samples were confirmed by powdered X-ray diffractometry (XRD; PANalytical X'Pert PRO) with Cu Kα ($\lambda = 0.154$ nm) radiation and transmission Fourier-transform infrared (FT-IR; Bruker IFS-28) spectroscopy. Whereas, their sulfur and metal contents were determined by ICP-MS (Jarrell-Ash, ICP 9000) elemental analyses and their BET surface areas were determined by N_2 adsorption/desorption measurements (Micromeritics ASAP 2010) done at 77 K.

2.2. Acidity characterization

As mentioned earlier, the acid properties of the parent ZrO_2, SZ and M/SZ catalysts were characterized by different methods, namely ^{31}P MAS NMR of adsorbed TMPO, FT-IR spectroscopy of adsorbed pyridine (pyidine-IR) and temperature-programmed desorption of ammonia (NH_3-TPD). All ^{31}P MAS NMR spectra were acquired at a Larmor frequency of 202.46 MHz (Bruker MSL-500P) using a single pulse sequence under the following conditions: pulse-width, 2 μs; recycle delay, 10 s; sample spinning rate, 12 kHz. Aqueous 85% H_3PO_4 solution was used as external reference for the ^{31}P NMR chemical shift. Prior to the NMR experiment, each sample was subjected to dehydration treatment at 623 K for 48 h under vacuum (10^{-5} Torr). Detailed procedures involved in introducing the TMPO probe molecule onto the catalyst sample can be found elsewhere [27,45–47]. To afford quantitative determination of acid sites, each TMPO-loaded sample was also subjected to element analysis by ICP-MS.

Supplementary acidity information was also acquired by pyridine-IR and NH_3-TPD studies. Prior to each IR experiment, compressed sample (in form of a self-supporting wafer, ca. 6 mg/cm^2) placed in the IR cell (with ZnSe windows) was first subjected to evacuation treatment at 673 K for 3 h, followed by saturated adsorption of pyridine at room temperature (RT; 298 K) for 1 h and subsequent removal of physisorbed pyridine under vacuum at 423 K overnight. Each FT-IR spectra was acquired by scanning from 4000 to 900 cm^{-1} (resolution of

2 cm^{-1}); 16 repeated scans were accumulated. NH_3-TPD experiments were carried out on a chemisorption apparatus (Micromeritics; AutoChem II 2920) equipped with a TCD detector. Prior to the adsorption of NH_3, ca. 100 mg sample was first preheated at 383 K under flowing He for 0.5 h to remove undesirable physisorbed species, followed by heating under He environment at 873 K for 1 h, then cooled to 393 K. Subsequently, the sample was exposed to flowing ammonia gas mixture (5% NH_3 in He) for 1 h, then purged by He gas for 40 min to remove excessive physisorbed ammonia. All NH_3-TPD profiles were carried out by ramping the temperature from 393 to 873 K at a rate of 10 K/min.

3. Results and discussion

3.1. Structure characterization

The sulfur and metal contents obtained for various SZ-*x*N (*x* = 0.5, 1.0 and 2.0) and M/SZ (M = Al, Ga and Fe) samples by ICP-MS are depicted in Table 1 along with their corresponding BET surface areas derived from N_2 adsorption/desorption measurements. Accordingly, a sulfur content of 1.4, 1.8 and 2.8 wt.% was observed for SZ-0.5N, SZ-1.0N and SZ-2.0N sample, respectively. On the other hand, while a respective metal loading of 1.1, 1.4 and 0.8 wt.% was found for Al/SZ, Ga/SZ and Fe/SZ, these M/SZ samples all exhibit an expected sulfur content of 1.8 ± 0.2 wt.%, similar to their parent SZ-1.0N. Furthermore, an apparent increase in BET surface area was found in the modified (SZ-*x*N and M/SZ) samples compared to their parent ZrO_2, indicating that the elaborated sulfation treatment leads to conspicuous changes in its physical properties, in accordance with previous studies [50].

It is well known that pure ZrO_2 may have two coexisting structurally stable phases, namely monoclinic and tetragonal phases; whose distributions largely depend on the calcination temperature during which the material is being prepared [3,49]. For example, Song and Sayari [3] disclosed that calcination of pure $Zr(OH)_4$ at 823 K resulted in formation of ZrO_2 with coexisting tetragonal and monoclinic phases. Upon increasing the calcination temperature, the tetragonal phase gradually diminished while the monoclinic phase increased, whereas when the temperature is above 923 K, only the monoclinic phase was observed. However, the authors also revealed that, after sulfation treatment, the SZ catalyst calcined at a temperature range of 823–973 K exists only tetragonal phase. It is only when the calcination temperature is above 1073 K that the formation of monoclinic phase became more evident. Thus, it is indicative that sulfation treatment promotes stabilized formation of the tetragonal phase in ZrO_2.

The XRD patterns of the parent ZrO_2, SZ and M/SZ samples are displayed in Fig. 1. Unlike the parent ZrO_2 sample, which reveals the coexistence of monoclinic (M) and tetragonal (T) phases (Fig. 1a), all SZ and M/SZ samples (which were calcined at 873 K) exhibit characteristic peaks at 2θ of 30°, 35°, 50° and 60° (Fig. 1a and b), indicating the presence of only the tetragonal phase. Moreover, incorporation of metal promoter does not affect the structural phase of SZ. The presence of the

Table 1
List of chemical compositions and BET surface areas for various SZ and M/SZ samples

Sample	Description	Content (wt.%)[a]		BET surface area (m^2/g)[b]
		S	Metal	
ZrO_2	Parent zirconia	–	–	36
SZ-0.5N	SZ (0.5N sulfuric acid)	1.4	–	127
SZ-1.0N	SZ (1N sulfuric acid)	1.8	–	117
SZ-2.0N	SZ (2N sulfuric acid)	2.8	–	110
Al/SZ	Al_2O_3 promoted SZ-1.0N	1.8	1.1	128
Ga/SZ	Ga_2O_3 promoted SZ-1.0N	2.0	1.4	124
Fe/SZ	Fe_2O_3 promoted SZ-1.0N	1.7	0.8	115

[a] Data obtained from ICP-MS.
[b] Data obtained from N_2 adsorption/desorption measurements at 77 K.

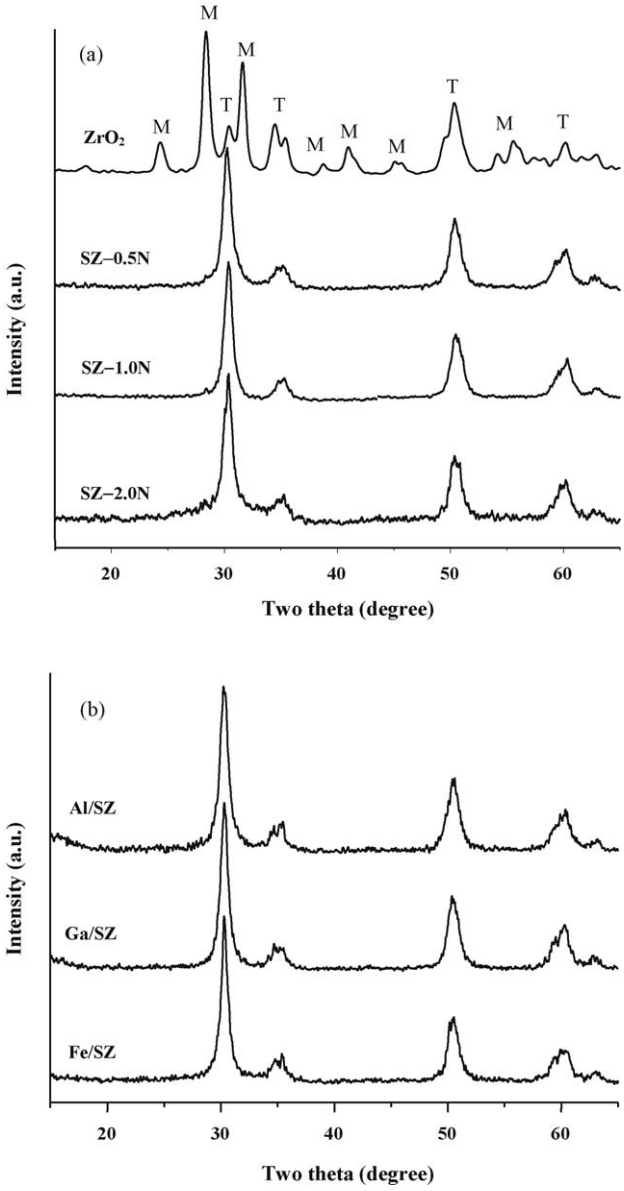

Fig. 1. XRD patterns of (a) pure ZrO_2 and various sulfated zirconia (SZ-*x*N; *x*, 0.5, 1.0 and 2.0) prepared with varied sulfur contents and (b) various metal-promoted sulfated zirconia (M/SZ; M = Al, Ga and Fe).

tetragonal phase in SZ and/or M/SZ, however, is known to facilitate the high activity observed during catalytic reactions at low temperature [1–3]. It is worth mentioning that our separate experiments performed on various as-synthesized SZ and M/SZ samples by using diffuse reflectance FT-IR (DRIFT) confirmed the existence of IR bands (not shown) due to S−O asymmetric and symmetric vibrations (990–1285 cm^{-1}) and Zr−O vibrations (415–750 cm^{-1}). Upon further dehydration treatment at 673 K, characteristic IR bands corresponding to Zr−OH vibrations on ZrO_2 (3760 and 3660 cm^{-1}) and on SO_4^{2-}−ZrO_2 (3640 cm^{-1}) [28] were observed. The above results thus verify that the SZ and M/SZ catalysts synthesized and used herein indeed possess the desirable structural and physical properties.

3.2. Acidity characterization by ^{31}P MAS NMR of adsorbed TMPO

^{31}P MAS NMR was invoked to characterize the acid features of various SZ and M/SZ catalysts using the adsorbed TMPO as the probe molecule. Accordingly, the ^{31}P MAS NMR spectra obtained from various TMPO-loaded samples are shown in Figs. 2 and 3, their chemical shifts, distributions and concentrations of acid sites derived in conjunction with elemental analyses by ICP-MS are depicted in Table 2. As expected, the ^{31}P NMR chemical shifts observed for TMPO adsorbed on Brønsted and Lewis acid sites of various SZ and M/SZ catalysts span over a chemical shift rage of 50–100 ppm, which is typical for solid acid catalysts [27,43–47]. The assignments of ^{31}P NMR resonances, namely their chemical shifts and relative distributions (i.e., their corresponding integrated areas) in each spectrum (Figs. 2 and 3) were achieved by simulation using the Gaussian deconvolution method. A Win-NMR software program (Bruker Biospin) allowed for curve fitting through appropriate choices of ^{31}P NMR peaks based on the observed resonance lineshape. Consequently, when all resonance peaks, each (assuming a Gaussian lineshape) in the proximity of a particular spectral position corresponding to an error in chemical shift value of ±2 ppm, resulted in a simulated spectrum nearly identical to the observed spectrum is considered a high quality fit. As such, specific chemical shifts and corresponding integrated areas in each spectrum can be determined with minimal ambiguities especially under experienced simulation skills. For example, spectral simulation of the result observed for the parent ZrO_2 in Fig. 2a (top spectrum) revealed that there are four distinct resonance peaks (as indicated by dashed curves), respectively located at ^{31}P NMR chemical shift of 62, 53, 41 and 34 ppm. The latter two peaks with chemical shifts lower than 50 ppm can be unambiguously assigned due to physisorbed TMPO and hence are irrelevant with the acid features of the catalyst sample being examined. The other two peaks at higher chemical shifts (62 and 53 ppm), however, are most likely due to TMPO adsorbed on Brønsted (B) and/or Lewis (L) acid sites. Clearly, this notion deserves further justifications, as will be discussed below.

It is known that Lewis acid sites (L-sites) may easily react with water to form Brønsted acid sites (B-sites). On the other hand, upon adsorption of TMPO probe molecule, the strong

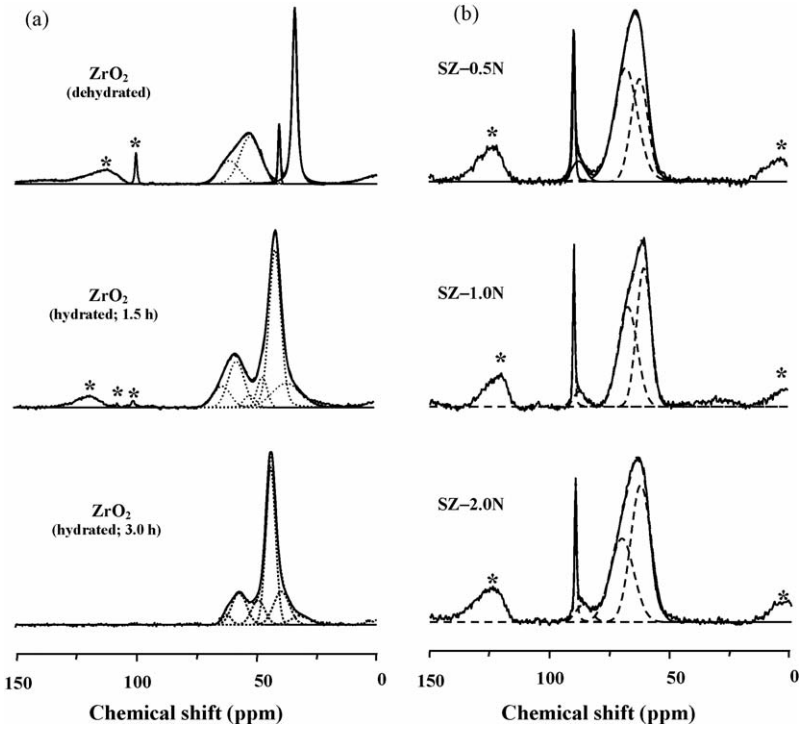

Fig. 2. ^{31}P MAS NMR spectra of TMPO adsorbed on (a) dehydrated pure ZrO_2 before (top) and after hydration treatments for 1.5 h (middle) and 3.0 h (bottom), and (b) dehydrated SZ-*x*N (*x* = 0.5, 1.0 and 2.0) prepared with varied sulfur contents. The dashed curves represent spectral simulation results and the asterisks denote spinning sidebands (spinning rate 12 kHz).

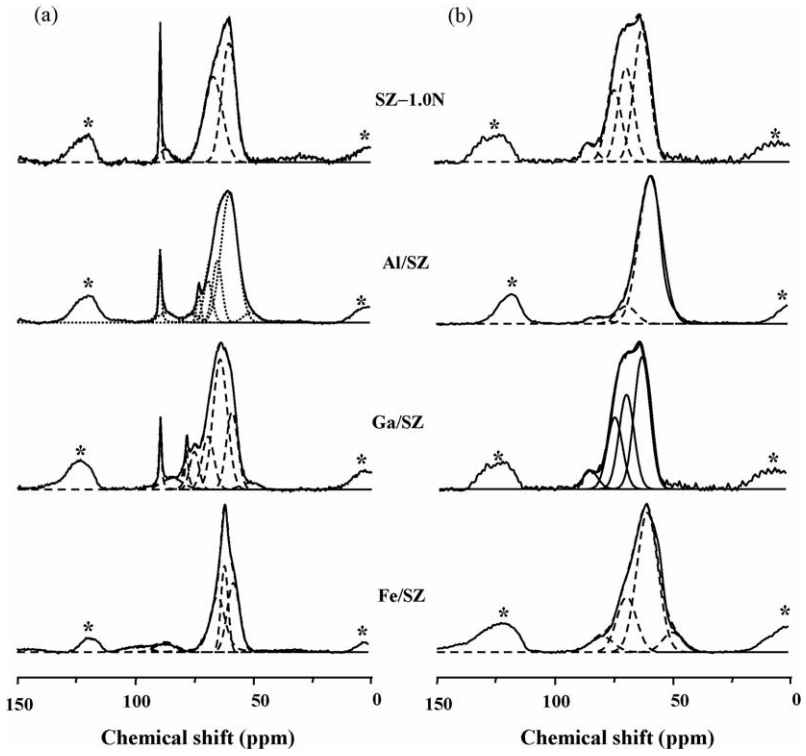

Fig. 3. ^{31}P MAS NMR spectra of TMPO adsorbed on dehydrated M/SZ (M = Al, Ga and Fe) (a) before and (b) after hydration treatment (for 1 h). The dashed curves represent spectral simulation results and the asterisks denote spinning sidebands (spinning rate 12 kHz).

hydrogen bonds between TMPO and B-sites are unlikely to be dissociated while in the presence of H_2O. Consequently, only those ^{31}P resonances associated with L-sites will be diminished upon further hydration of the sample. Indeed, upon progressive exposure of the TMPO-loaded ZrO_2 sample to humidity, the peak intensities at 62 and 53 ppm decrease with increasing water content while their chemical shifts remain practically unchanged. Meanwhile, the peaks responsible for physisorbed TMPO at 41 and 34 ppm are broadened and shifted toward downfield (i.e., higher chemical shift) direction. Accordingly, the two peaks at 62 and 53 ppm observed for the parent ZrO_2 sample can hence be ascribed due to interaction of TMPO with two different (weak; see below) L-sites. These results are in excellent agreement with earlier reports [28,29,51] studied by IR spectroscopy of adsorbed CO, by which two types of L-sites exhibiting different acid concentrations, strengths and stabilities were identified for pure ZrO_2.

It has been shown that, upon loading the TMPO adsorbate onto an acid catalyst, the base probe molecule tends to form hydrogen bonding with the acid sites [27,43]. Consequently, the density of the electron cloud surrounding the ^{31}P nucleus neighboring to the oxygen atom on the phosphine oxides decreases with increasing strength of the acid sites, which in turn causes the ^{31}P resonance to shift towards downfield (higher chemical shift) direction. In other words, ^{31}P NMR resonance having a higher chemical shift should reflect sites that possess a higher acidic strength.

Fig. 2b displays the ^{31}P MAS NMR spectra of TMPO adsorbed on SZ samples prepared with different sulfur contents. Unlike the parent ZrO_2 sample, the TMPO-loaded SZ-xN (x = 0.5, 1.0 and 2.0) samples all reveal four distinct ^{31}P resonance peaks at 90, 87, 68 and 63 ppm (Table 2). The abnormal sharp resonance at 90 ppm, which has never been observed before in solid acid catalysts, demands further justification. More discussion on the assignment (origin) of this resonance peak will be made later. Most intriguingly, upon incorporation of promoted metal (M = Al, Ga and Fe) onto the source SZ-1.0N material, several new resonance peaks emerged in the M/SZ catalysts, as shown in Fig. 3a. For examples, both the TMPO-loaded Al/SZ and Ga/SZ samples exhibit a total of eight ^{31}P resonance peaks in which four of them have identical chemical shifts with those found in their parent counterpart, SZ-1.0N. Whereas for the Fe/SZ sample, which was prepared by a slightly different method, up to six resonance peaks were observed in which only three of them were existed in SZ-1.0N (see Fig. 3a; Table 2).

Nevertheless, before going any further to explore the explicit reasons for the observed emergence and/or collapse of these resonance peaks, we must first clarify the natures (i.e., types) of acid sites involved. This, again, can be accomplished by performing additional experiments on hydrated samples. The ^{31}P MAS NMR spectra obtained from TMPO-loaded M/SZ samples after subjecting to hydration treatment (by exposing to humility for 1 h) are shown in Fig. 3b. Accordingly, proper assignments regarding to the genuine types of acid sites can be made. By comparing the spectra in Fig. 3b with that obtained from the corresponding as-synthesized (dehydrated) M/SZ samples shown in Fig. 3a, it is clear that resonance peaks at 99 (only for Fe/SZ sample), 90 and 73 ppm were diminished after the hydration treatment. Thus, these peaks can be

Table 2
^{31}P MAS NMR chemical shift assignments and distribution of acid sites for various SZ and M/SZ samples loaded with TMPO probe molecule

Sample	Chemical shift (ppm)[a,b]										Acid amount (mmol/g cat.)[c]			
	[99]	[90]	87	76	[73]	68	65	[62]	[53]	P[c]	Brønsted	Lewis	Total	B/L (%)
ZrO_2	–	–	–	–	–	–	–	50.3%	49.7%	✓	–	–	–	–
SZ-0.5N	–	7.9% (0.003)	5.4% (0.002)	–	–	53.3% (0.023)	–	33.4% (0.015)	–	–	0.025	0.018	0.043	1.39
SZ-1.0N	–	7.4% (0.012)	3.7% (0.006)	–	–	43.2% (0.071)	–	45.7% (0.075)	–	–	0.077	0.087	0.164	0.89
SZ-2.0N	–	6.0% (0.005)	5.1% (0.004)	–	–	37.2% (0.028)	–	51.7% (0.039)	–	–	0.032	0.044	0.076	0.73
Al/SZ	–	5.3% (0.008)	4.3% (0.006)	2.8% (0.004)	3.1% (0.005)	9.7% (0.015)	15.3% (0.023)	55.8% (0.084)	3.7% (0.006)	–	0.048	0.103	0.151	0.47
Ga/SZ	–	4.1% (0.005)	5.5% (0.007)	3.5% (0.005)	7.8% (0.010)	14.4% (0.019)	41.9% (0.054)	20.0% (0.026)	2.8% (0.004)	–	0.085	0.045	0.130	1.89
Fe/SZ	4.5% (0.013)	–	6.3% (0.018)	–	–	12.9% (0.038)	13.7% (0.040)	27.0% (0.079)	35.6% (0.105)	✓	0.096	0.197	0.293	0.49

[a] For comparison, simulation results (see text) obtained for various samples representing TMPO adsorbed on Brønsted and/or Lewis (denoted by chemical shift values in brackets) acid sites with practically the same chemical shift (i.e., similar acid strengths) are aligned in the same column.
[b] For SZ-xN (x = 0.5, 1.0 and 2.0) and M/SZ (M = Al, Ga and Fe) samples, data denote relative concentration of acid sites (%); whereas data in parentheses represent acid concentration (±0.002 mmol/g cat.) of the corresponding acid site, as derived from elemental analyses by ICP-MS.
[c] Resonance peaks with chemical shift lower than 50 ppm (see Figs. 2 and 3), which arise from physisorbed TMPO, are excluded during derivations of acid amount [27,46].

unambiguously attributed to TMPO adsorbed on L-sites. As such, all resonance peaks observed for the parent ZrO_2 (Fig. 2a) and various SZ (Fig. 2b) and M/SZ (Fig. 3a) catalysts can be assigned individually, as listed in Table 2. More specifically, resonances at chemical shifts of 99, 90, 73, 62 and 53 ppm are assigned due to Lewis acid sites; they are denoted by values in brackets in Table 2, whereas peaks at 87, 76, 68 and 65 ppm are associated with TMPO adsorbed on Brønsted acid sites. As mentioned earlier, resonance with a higher chemical shift value corresponds to Brønsted and/or Lewis acid sites that possess higher acidic strengths. It is also noted that, resonance peaks having practically the same chemical shifts (i.e., acid sites with similar acidic strength) in different catalyst samples are aligned in the same column in Table 2 for comparison purpose. Thus, the strongest L-sites found in SZ and M/SZ are at 99 (only for Fe/SZ) and 90 ppm, likewise, the strongest B-sites correspond to the peak located at 87 ppm.

Additional quantitative information of the acid sites can be derived by incorporating results obtained from elemental analyses of S, Zr, Al, Ga, Fe and P by ICP-MS, the results are also depicted in Table 2. The acid amount (in mmol/g cat.) of each corresponding B- or L-sites can thus be derived using the re-normalized (i.e., after excluding contribution arising from physisorbed TMPO) relative concentrations obtained from spectral simulation by Gaussian deconvolution based on the assumption that each TMPO molecule can only be adsorbed on either one Brønsted or Lewis acid site [27,46], that is, the TMPO adsorbate and the acid site are on 1:1 basis.

Next, let's discuss the variations of relative integrated areas of the ^{31}P resonances, which reflect relative concentrations of the corresponding acid sites (see below) having the same acid strength. These values can readily be derived by the results obtained from spectral simulation of the corresponding sample. A closer examination of the ^{31}P MAS NMR results displayed in Table 2 leads to some interesting findings, which can be summarized below:

(i) The pure ZrO_2 sample possesses only two types of weak L-sites (at 62 and 53 ppm); no evidences associated with the presence of B-sites were to be found.
(ii) Upon sulfation treatment of the parent ZrO_2 by sulfuric acid with varied concentrations (x = 0.5, 1.0 and 2.0N), coexisting L-sites (at 90 and 62 ppm) and B-sites (at 87 and 68 ppm) in SZ-xN samples were observed. In particular, the emergences of the strong L-sites (at 90 ppm) as well as B-sites with strong (87 ppm) and medium (68 ppm) acid strengths took place mostly at the expanses of the weak L-sites originally existed in ZrO_2, particularly the one with weaker strength (at 53 ppm), which diminishes upon sulfation treatment. Moreover, while the SZ-xN catalysts were all found to exhibit the existence of pure tetragonal phase, a maximum Brønsted, Lewis and total acidities were found on sample sulfated with a sulfuric acid concentration (x) of 1.0N.
(iii) Upon incorporation of ca. 1.0 wt.% of promoted Al or Ga metals onto the SZ-1.0N catalyst, both TMPO-loaded Al/SZ and Ga/SZ samples exhibit a total of eight ^{31}P

resonance peaks, in which four of them have identical chemical shifts with those found in their parent SZ-1.0N catalyst. The appearances of the extra B-sites (76 and 65 ppm) and L-sites (73 and 53 ppm), whose acid strengths span over both medium and weak regimes, occur mostly at the disposals of the strongest L-sites (90 ppm) and medium B-sites (68 ppm) acid sites in SZ-1.0N. Whereas for Fe/SZ catalyst, formations of a very strong (99 ppm) and a very weak L-sites (53 ppm) as well as the notable increase in the strong (87 ppm) and an additional weak (65 ppm) B-sites were observed, mostly at the collaborative costs of the strong (90 ppm) and weak (62 ppm) L-sites and medium B-sites (68 ppm) of its parent SZ-1.0N sample.

(iv) In terms of the *overall* acidity, the following trends can be inferred for SZ-*x*N ($x = 0.5$, 1.0 and 2.0) catalysts with different sulfur contents:

$$\text{Brønsted acidity}: \text{SZ-1.0N} \gg \text{SZ-2.0N} > \text{SZ-0.5N} \gg \text{ZrO}_2\ (\text{null});$$

$$\text{Lewis acidity}: \text{SZ-1.0N} > \text{SZ-2.0N} > \text{SZ-0.5N};$$

$$\text{B/L ratio}: \text{SZ-0.5N} > \text{SZ-1.0N} > \text{SZ-2.0N} \gg \text{ZrO}_2\ (\text{null});$$

$$\text{Total acidity}: \text{SZ-1.0N} \gg \text{SZ-2.0N} > \text{SZ-0.5N}.$$

Whereas, comparing to their source SZ-1.0N sample, the following trends for M/SZ (M = Al, Ga and Fe) catalysts prevail:

$$\text{Brønsted acidity}: \text{Fe/SZ} > \text{Ga/SZ} > \text{SZ-1.0N} \gg \text{Al/SZ};$$

$$\text{Lewis acidity}: \text{Fe/SZ} \gg \text{Al/SZ} > \text{SZ-1.0N} > \text{Ga/SZ};$$

$$\text{B/L ratio}: \text{Ga/SZ} \gg \text{SZ-1.0N} > \text{Fe/SZ} \approx \text{Al/SZ};$$

$$\text{Total acidity}: \text{Fe/SZ} \gg \text{SZ-1.0N} > \text{Al/SZ} > \text{Ga/SZ}.$$

The aforediscussed findings are mostly in accordance with existing literature reports studied by various methods. For example, by means of the combined IR, frequency response (FR) and TPD techniques using NH_3 as the probe molecule, Barthos et al. [19] revealed that SZ contains two types of L-sites of distinctly different acid strengths as well as B-sites with broad distribution of acid strengths. Davis et al. [33] performed a series of studies on Pt/SZ and SZ catalysts by pyridine-IR, and reported a B/L ratio of ca. 0.8–1.0 for a SZ sample prepared by using 1N H_2SO_4 (similar to the SZ-1.0N sample reported herein). Furthermore, Gao et al. [14,15] disclosed that abundant distribution of acid sites with intermediate strengths are responsible for the remarkable activity and stability observed for Al/SZ catalyst during *n*-butane isomerization reaction. Through microcalorimetric measurements of adsorbed NH_3, the authors further demonstrated that the acid sites in the Al/SZ catalysts are inhomogeneously distributed. Moreno and Poncelet [12] reported that Ga/SZ has a better catalytic performance than Al/SZ and that these promoted catalysts all exhibited higher fractions of tetragonal structure, sulfate density and Brønsted acidity with respect to SZ. The aforementioned studies provide additional supports to the results presented herein. Among the various M/SZ catalysts examined in this study, the Fe/SZ sample is found to possess a high Brønsted, Lewis and *total* acidity. On the other hand, Ga/SZ tends to possess more Brønsted acid sites but less Lewis acid sites compared to Al/SZ. Obviously, incorporation of different metal promoters onto SZ not only resulted in additional formation of B- and L-sites but also leads to variations among different acid sites. In particular, formations of extraordinary strong L-sites (at 99 ppm) and strong B-sites (at 87 ppm) were observed for Fe/SZ catalyst compared to SZ-1.0N and its metal-promoted counterparts. It has been suggested that the promoted Fe metal may be associated with a larger number of catalytic centers and high acid strength of the acid sites compared to SZ [6].

3.3. Acidity characterization by pyridine-IR spectroscopy and NH_3-TPD

To afford additional supports to the results obtained from ^{31}P MAS NMR discussed above, more experiments were carried out to characterize the acid properties of various samples using pyridine-IR and NH_3-TPD techniques. FT-IR spectroscopy of adsorbed pyridine is a useful technique commonly used for discernment of Brønsted and Lewis acid sites. The adsorbed pyridine probe molecules tend to couple with aprotic (Lewis) and/or protonic (Brønsted) catalytic centers through the nitrogen lone-pair electrons and hence can be detected by monitoring their ring vibrations. The FT-IR spectra of pyridine adsorbed on various SZ-*x*N samples in Fig. 4 reveal characteristic bands in the range of 1400–1650 cm^{-1}. In general, the bands at 1545 and 1455 cm^{-1} can be assigned due to B- and L-sites, respectively, whereas the band at 1495 cm^{-1} is normally attributed to a combination band associated with both B- and L-sites [29]. Obviously, the IR spectrum observed for the pure ZrO_2 sample exhibits only vibrational bands associated with L-sites (at 1455 and 1607 cm^{-1}), whereas coexistence of B-sites (at 1545 and 1640 cm^{-1}) and L-sites (at 1455 and 1607 cm^{-1}) are evident for SZ-*x*N samples in addition to the combination band at 1495 cm^{-1}. This implies generation of B-sites during the sulfation treatment of ZrO_2, in excellent agreement with the findings by ^{31}P MAS NMR of adsorbed TMPO.

Nevertheless, acidity characterization by pyridine-IR technique is limited by the drawback in only capable of providing qualitative information (i.e., types) of acid sites. As such, it is normally combined with NH_3-TPD study, which can provide additional qualitative information regarding to the *overall* concentration and strength of the acid sites. The NH_3-TPD profiles for various SZ and M/SZ catalysts are shown in Fig. 5. Pure ZrO_2 shows one broad low-temperature (LT) desorption peak at about 453 K which is attributed to NH_3 adsorbed on weak L-sites, whereas samples after sulfation (SZ-*x*N; $x = 0.5$, 1.0 and 2.0) reveal the generation of broad medium-temperature (MT) desorption signals (at the range of 473–723 K) corresponding to NH_3 adsorbed on acid sites with medium strengths and a distinct high-temperature (HT) peak at ca. 800 K suggesting the presence of very strong acid sites

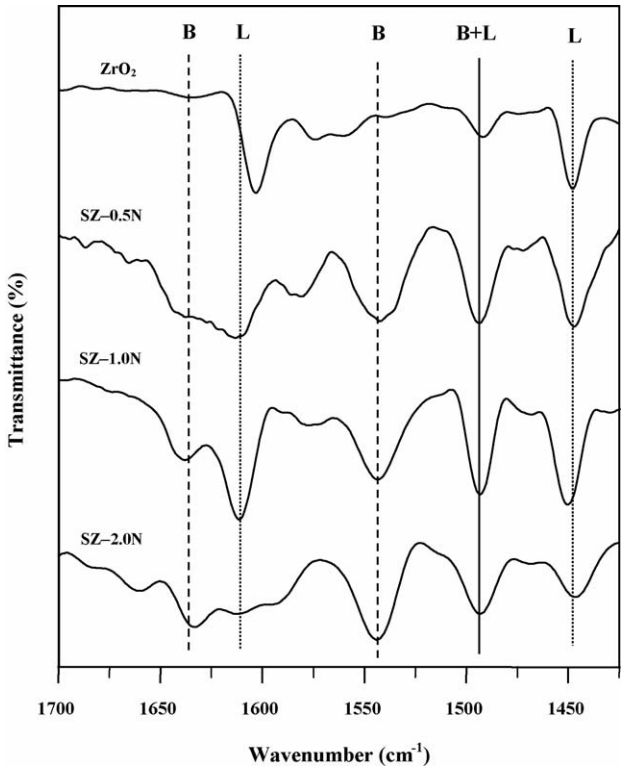

Fig. 4. FT-IR spectra of pyridine adsorbed on pure ZrO_2 and SZ-*x*N ($x = 0.5$, 1.0 and 2.0) prepared with varied sulfur contents.

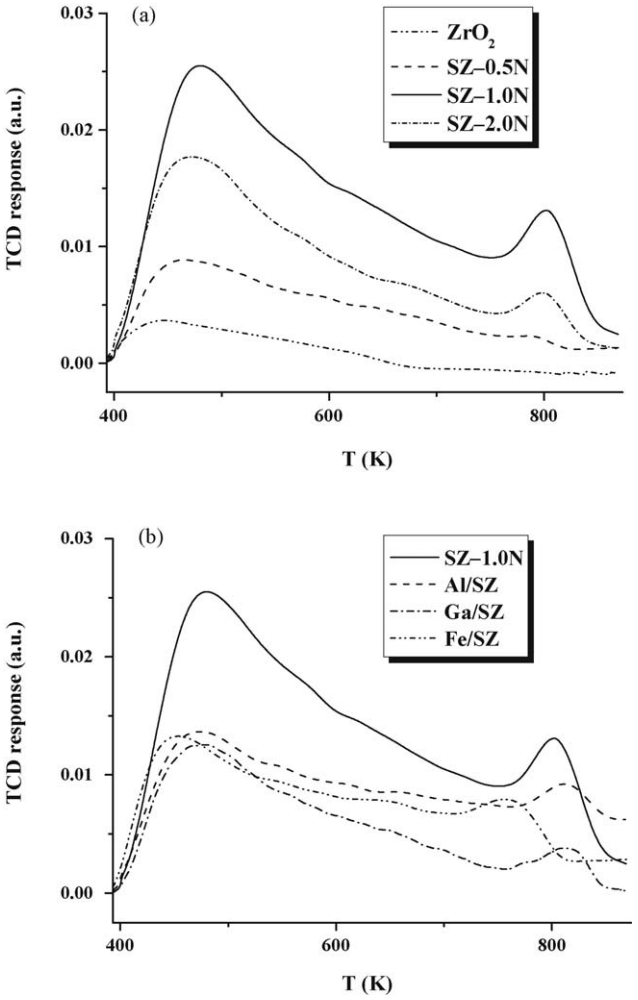

Fig. 5. NH_3-TPD profiles of (a) pure ZrO_2 and SZ-*x*N ($x = 0.5$, 1.0 and 2.0) prepared with varied sulfur contents and (b) SZ-1.0N and M/SZ (M = Al, Ga and Fe).

(Fig. 5a). It is indicative that, after the sulfation treatment, the acid sites in SZ-*x*N samples are not homogeneously distributed and hence resulting a broad distribution of acid sites with weak, medium and high acid strengths. Nevertheless, one can still make justifiable comment on the *overall* acid strengths for ZrO_2 and SZ-*x*N samples based on the NH_3-TPD results (Fig. 5a), which appear to obey the following trend:

$$\text{SZ-1.0N} \gg \text{SZ-2.0N} > \text{SZ-0.5N} \gg ZrO_2.$$

Furthermore, the *overall* acid amounts in various ZrO_2 and SZ-*x*N samples can also be inferred from the relative peak areas of the NH_3 desorption curves, which appear to have the same trend for the *overall* acid strength above as well as that of *total* acidity observed by solid-state ^{31}P MAS NMR of adsorbed TMPO (derived in junction with ICP-MS results; see Section 3.2 above). It is indicative that elaborated sulfation treatment made on pure ZrO_2 not only led to conspicuous changes in its structural and physical properties, but also a significant increase in its acidity.

By the same token, the *overall* acid amounts for SZ-1.0N and M/SZ catalysts (Fig. 5b) can also be inferred, which seem to follow the trend:

$$\text{SZ-1.0N} \gg \text{Al/SZ} \approx \text{Fe/SZ} > \text{Ga/SZ}.$$

The above results based on NH_3-TPD experiments indicate that promotion of metal on to SZ resulted in a notable decrease in *overall* acidity. Moreover, in terms of acid strength, while all M/SZ samples revealed similar LT desorption peaks, they are located at a temperature lower than that of SZ-1.0N. Similar to SZ-*x*N samples, HT desorption peak was also observed for M/SZ catalysts, indicating the presence of 'very strong' acid sites. It is intriguing to find that the temperatures at which the HT desorption peak occur in Al/SZ and Ga/SZ are slightly higher than their source SZ-*x*N sample, however, an opposite trend was found for Fe/SZ. These observations deserve further verification. The above observations based on the NH_3-TPD results are clearly against those obtained from the combined ^{31}P NMR and ICP-MS studies, by which a pronounced increase in *total* acidity was observed for Fe/SZ compared to SZ-1.0N (see Section 3.2 above). While the reasons responsible for such discrepancies remain to be clarified, it is noted that the NH_3-TPD method invokes detection of acid sites through titration of adsorbed NH_3, which may provoke couplings and/or bonding between the N atom on the NH_3 probe molecule and OH groups associated with sulfur and/or metal promoters of the SZ and M/SZ catalysts, hence led to additional complexity in terms of interpretation of the experimental results.

The presence of HT desorption peaks, which represents desorption of NH_3 on 'very strong' acid sites should be subjects of particular interests, have been observed previously in various SZ and sulfated mixed oxides catalysts [4,14,16,26,29,35,50,52–

54]. For example, Das et al. [26] reported a relevant study on Fe- and Mn-promoted sulfated zirconia-titania mixed oxide catalysts by means of temperature programmed reduction (TPR) experiments. They observed a broad, asymmetric HT desorption peak spanning from 773 to 1023 K on the parent SO_4^{2-}/ZrO_2-TiO_2 catalyst that was claimed due to emergences of two overlapped peaks; one broad peak whose onset begins at ca. 573 K with peak maximum at 948 K and another sharp peak with peak maximum at ca. 1000 K. The authors attributed the broad peak to relatively less stable sites and the sharp peak to more stable surface sulfate species. Upon promoted by metal, the sulfate reduction peaks were observed at relatively lower temperatures, suggesting an enhancement of sulfate reduction in presence of metal ions. Moreover, the reduction peaks observed for Fe-promoted sample were both found to occur at temperatures (803 and 853 K) ca. 150 K lower than that of parent and Mn-promoted SO_4^{2-}/ZrO_2-TiO_2. The authors suggested that this is due to the fact that the surface sulfate groups are less stable in presence of Fe over ZrO_2-TiO_2 surface, as evidenced by their results from TPR studies.

To verify the HT desorption peaks observed for SZ-*x*N and M/SZ catalysts, additional experiments were performed by preheating the SZ-2.0N catalyst from RT to 1073 K in flowing dry He gas prior to recording of the TCD signal. The resultant TPD profile revealed two desorption peaks at 368 and 923 K, as shown in Fig. 6a. The former peak can be assigned due to water desorption and the latter due to decomposition of SO_4^{2-} Subsequently, NH_3-TPD profiles of the same sample subjected to two different preheating temperatures (1073 and 873 K) were recorded after loading the NH_3 adsorbate, as shown in Fig. 6b and c, respectively. Unlike the NH3-TPD profile of the sample pretreated at elevated temperature (1073 K), which shows only the LT desorption peak with very weak intensity (Fig. 6b), two distinct peaks were observed for the same sample pretreated at 873 K. Clearly, the emergences of the LT (at 473 K) and HT (at 798 K) peaks observed in the latter sample (Fig. 6c) are due to NH_3 desorbed from weak and strong acid sites, respectively,

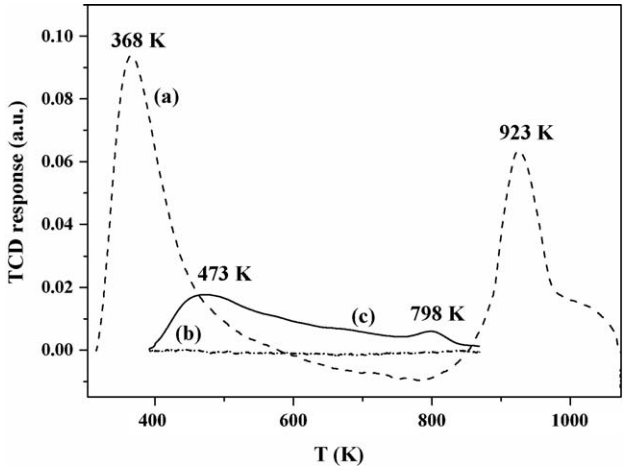

Fig. 6. (a) TPD profile of SZ-2.0N sample subjected to (a) preheating from room temperature (293 K) to 1073 K under flowing He gas and NH_3-TPD profiles of the same sample subjected to different pretreatment temperatures at (b) 1073 K and (c) 873 K prior to NH_3 adsorption.

rather than dissociation of SO_4^{2-}. Previous ^{1}H MAS NMR [17] and theoretical calculations [29] studies suggested that the 'very strong' acid sites or 'superacidity' found in SZ and M/SZ are mostly due to the presence of Brønsted acid sites. In contrast, other investigations by IR, TPD and calorimetric studies based on varied adsorbed base probe molecules [19,54] revealed the strongest acid sites are associated with Lewis acidity. In this context, the fact that all SZ-*x*N and M/SZ catalysts examined herein exhibit a HT desorption peak (above ca. 800 K) in the NH_3-TPD profiles (Fig. 5) and show more total Lewis acidity than Brønsted acidity (except for Ga/SZ) with high acid strengths (Table 2) in the corresponding ^{31}P MAS NMR spectrum indicate that the 'very strong' acid sites induced by the surface sulfate species with high degree of unsaturated electrons should arise most due to Lewis acidity. An exception is found for Ga/SZ in which more Brønsted acidity was found than Lewis acidity. In other words, it may be concluded that, except for Ga/SZ, the 'very strong' acidities observed in sulfated and metal-promoted zirconia oxides are mainly due to the higher concentration of L-sites than B-sites with higher acid strengths.

4. Conclusions

We have demonstrated that detailed acid properties and variations of acid sites of various sulfated and metal-promoted zirconia catalysts can be achieved by using the combined technique invoking ^{31}P MAS NMR spectroscopy of adsorbed TMPO as the probe molecule and elemental analysis by ICP-MS. It is found that elaborated sulfation and subsequent calcination (at 873 K) treatments of pure ZrO_2, which possesses coexistence of monoclinic and tetragonal structural phases, tends to promote formation of sulfated zirconia (SZ) catalysts with pure tetragonal phases and higher BET surface areas. Moreover, while the parent ZrO_2 possesses only two types of weak Lewis acid sites, coexistence of Brønsted and Lewis acid sites with higher acid strengths was observed for SZ-*x*N catalysts prepared by using different sulfuric acid concentrations (*x*). As a result, two types of Brønsted acid sites with strong and medium strengths and two types of Lewis acid sites with strong and weak strengths were identified. Nevertheless, the acid strengths of these acid sites were found independent of the sulfur contents. Further incorporation of ca. 1.0 wt.% metal promoters onto SZ resulted in additional formation of Brønsted and Lewis acid sites, In the case of TMPO-loaded Al/SZ and Ga/SZ catalysts, a total of eight ^{31}P distinct resonances corresponding to sites with different acid strengths were identified; those with chemical shifts at 90, 73, 62 and 53 ppm are ascribed due to Brønsted acidities, whereas those at 87, 76, 68 and 65 ppm are attributed to Lewis acidities. Among them, Ga/SZ was found to possess more Brønsted acid sites than Al/SZ, and vice versa for Lewis acidities. On the other hand, only three types of Brønsted acid sites (at 99, 62 and 53 ppm) and three types of Lewis acid sites (at 87, 68 and 65 ppm) were identified in Fe/SZ catalyst. Among them, a type of Lewis acid sties with very strong acid strength (at 99 ppm) was found for the first time in solid acid catalysts. Further elemental analyses

by ICP-MS confirmed that the total acidity obey the following trend for M/SZ's: Fe/SZ $\gg$ Al/SZ $>$ Ga/SZ, indicating the variances in promotion mechanisms of the incorporated metals. It has been shown that the 'very strong' acid sites observed for SZ-*x*N and M/SZ in this study should be associated more with Lewis acidity than Brønsted acidity, except for Ga/SZ, which is most likely dictated by the latter. Unlike conventional pyridine-IR and NH_3-TPD methods, which are only capable of providing qualitative information on the types and/or *overall* concentrations and strengths of acid sites, the unique combined ^{31}P MAS NMR and ICP-MS technique demonstrated herein not only renders simultaneous detections of detailed qualitative and quantitative information of acid sites but also allows for monitoring variations in strengths and concentrations among the corresponding acid sites upon sample sulfation and metal promotion treatments.

Acknowledgements

The supports of this work by the National Science Council, Taiwan (under Contract Nos.: NSC92-2113-M-001-049 and NSC93-2113-M-001-020; to SBL) are gratefully acknowledged.

References

[1] K. Tanabe, M. Misono, Y. Ono, H. Hatttori, Stud. Surf. Sci. Catal. 51 (1989) 199.
[2] A. Corma, Chem. Rev. 95 (1995) 559.
[3] X. Song, A. Sayari, Catal. Rev. Sci. Eng. 38 (1996) 329.
[4] G.D. Yadav, J.J. Nair, Micropor. Mesopor. Mater. 33 (1999) 1.
[5] K. Shimizu, N. Kounami, H. Wada, T. Shishido, H. Hattori, Catal. Lett. 54 (1998) 153.
[6] C.Y. Hsu, C.R. Heimbuch, C.T. Armes, B.C. Gates, J. Chem. Soc. Chem., Commun. (1992) 1645.
[7] F.C. Jentoft, A. Hahn, J. Kröhnert, G. Lorenz, R.E. Jentoft, T. Ressler, U. Wild, R. Schlögl, C. Häßner, K. Köhler, J. Catal. 224 (2004) 124.
[8] T.K. Cheung, J.L. D'itri, B.C. Gates, J. Catal. 151 (1995) 464.
[9] K. Föttinger, K. Zorn, H. Vinek, Appl. Catal. A 284 (2005) 69.
[10] P. Canton, R. Olindo, F. Pinna, G. Strukul, P. Riello, M. Meneghetti, G. Cerrato, C. Morterra, A. Benedetti, Chem. Mater. 13 (2001) 1634.
[11] V. Pârvulescu, S. Coman, V.I. Pârvulescu, P. Grange, G. Poncelet, J. Catal. 180 (1998) 66.
[12] J.A. Moreno, G. Poncelet, J. Catal. 203 (2001) 453.
[13] C.J. Cao, S. Han, C.L. Chen, N.P. Xu, C.Y. Mou, Catal. Commun. 4 (2003) 511.
[14] Z. Gao, Y. Xia, W. Hua, C. Miao, Top. Catal. 6 (1998) 101.
[15] W. Hua, Y. Xia, Y. Yue, Z. Gao, J. Catal. 196 (2000) 104.
[16] B. Umansky, J. Engelhardt, W.K. Hall, J. Catal. 127 (1991) 128.
[17] T. Riemer, D. Spielbauer, M. Hunger, G.A.H. Mekhemer, H. Knözinger, J. Chem. Soc., Chem. Commun. (1994) 1181.
[18] M. Hino, S. Kobayashi, K. Arata, J. Am. Chem. Soc. 101 (1979) 6439.
[19] R. Barthos, F. Lónyi, Gy. Onyestyák, J. Valyon, J. Phys. Chem. B 104 (2000) 7311.
[20] V. Adeeva, J.W. de Haan, J. Jänchen, G.D. Lei, V. Schünemann, L.J.M. van de Ven, W.M.H. Sachtler, R.A. van Santen, J. Catal. 151 (1995) 364.
[21] B.S. Klose, F.C. Jentoft, R. Schlögl, I.R. Subbotina, V.B. Kazansky, Langmuir 21 (2005) 10564.
[22] C.H. Lin, C.Y. Hsu, J. Chem. Soc., Chem. Commun. (1992) 1479.
[23] N. Satoh, J.I. Hayashi, H. Hattori, Appl. Catal. A 202 (2000) 207.
[24] P. Wang, S. Yang, J.N. Kondo, K. Domen, T. Yamada, H. Hattori, Chem. Lett. 32 (2003) 408.
[25] P. Wang, S. Yang, J.N. Kondo, K. Domen, T. Yamada, H. Hattori, J. Phys. Chem. B 107 (2003) 11951.
[26] D. Das, H.K. Mishra, A.K. Dalai, K.M. Parida, Catal. Lett. 93 (2004) 185.
[27] Q. Zhao, W.H. Chen, S.J. Huang, Y.C. Wu, H.K. Lee, S.B. Liu, J. Phys. Chem. B 106 (2002) 4462 (and references therein).
[28] L.M. Kustov, V.B. Kazansky, F. Figueras, D. Tichit, J. Catal. 150 (1994) 143.
[29] F. Babou, G. Coudurier, J.C. Vedrine, J. Catal. 152 (1995) 341.
[30] E.E. Platero, M.P. Mentruit, C.O. Areán, A. Zecchina, J. Catal. 162 (1996) 268.
[31] C. Morterra, G. Cerrato, S. Di Ciero, Appl. Surf. Sci. 126 (1998) 107.
[32] C. Morterra, G. Cerrato, F. Pinna, Spectrochim. Acta A 55 (1999) 95.
[33] B.H. Davis, R.A. Keogh, S. Alerasool, D.J. Zalewski, D.E. Day, P.K. Doolin, J. Catal. 183 (1999) 45.
[34] N. Katada, J.I. Endo, K.I. Notsu, N. Yasunobu, N. Naito, M. Niwa, J. Phys. Chem. B 104 (2000) 10321.
[35] R. Barthos, F. Lónyi, Gy. Onyestyák, J. Valyon, Solid State Ionics 141–142 (2001) 253.
[36] R. Olindo, A. Goeppert, D. Habermacher, J. Sommer, F. Pinna, J. Catal. 197 (2001) 344.
[37] J.R. Sohn, T.D. Kwon, S.B. Kim, Bull. Korean Chem. Soc. 22 (2001) 1309.
[38] D.J. Coster, A. Bendada, F.R. Chen, J.J. Fripiat, J. Catal. 140 (1993) 497.
[39] J.H. Lunsford, H. Sang, S.M. Campbell, C.H. Liang, R.G. Anthony, Catal. Lett. 27 (1994) 305.
[40] T. Riemer, H. Knözinger, J. Phys. Chem. 100 (1996) 6739.
[41] J. Zhang, J.B. Nicholas, J.F. Haw, Angew. Chem. Int. Ed. 39 (2000) 3302.
[42] J.F. Haw, J. Zhang, K. Shimizu, T.N. Venkatraman, D.P. Luigi, W. Song, D.H. Barich, J.B. Nicholas, J. Am. Chem. Soc. 122 (2000) 12561.
[43] E.F. Rakiewicz, A.W. Peters, R.F. Wormsbecher, K.J. Sutovich, K.T. Mueller, J. Phys. Chem. B 102 (1998) 2890.
[44] J.P. Osegovic, R.S. Drago, J. Phys. Chem. B 104 (2000) 147.
[45] W.H. Chen, T.C. Tsai, S.J. Jong, Q. Zhao, C.T. Tsai, H.K. Lee, I. Wang, S.B. Liu, J. Mol. Catal. A 181 (2002) 41.
[46] Q. Zhao, W.H. Chen, S.J. Huang, S.B. Liu, Stud. Surf. Sci. Catal. 145 (2003) 205.
[47] F. Bauer, W.H. Chen, H. Ernst, S.J. Huang, A. Freyer, S.B. Liu, Micropor. Mesopor. Mater. 72 (2004) 81.
[48] A. Sakthivel, N. Saritha, P. Selvam, Catal. Lett. 72 (2001) 225.
[49] T. Yamamoto, T. Tanaka, S. Takenaka, S. Yoshida, T. Onari, Y. Takahashi, T. Kosaka, S. Hasegawa, M. Kudo, J. Phys. Chem. B 103 (1999) 2385.
[50] A. Corma, V. Fornés, M.I. Juan-Rajadell, J.M. López Nieto, Appl. Catal. A 116 (1994) 151.
[51] V. Bolis, C. Morterra, M. Volante, L. Orio, B. Fubini, Langmuir 6 (1990) 695.
[52] E.C. Sikabwe, M.A. Coelho, D.E. Resasco, R.L. White, Catal. Lett. 34 (1995) 23.
[53] F. Lónyi, J. Valyon, J. Engelhardt, F. Mizukami, J. Catal. 160 (1996) 279.
[54] G. Yaluris, R.B. Larson, J.M. Kobe, M.R. González, K.B. Fogash, J.A. Dumesic, J. Catal. 158 (1996) 336.